Polymer Bulletin 61, 643–654 (2008)
DOI 10.1007/s00289-008-0979-6

Polymer Bulletin

Effect of cooling rate on melt-crystallization of random propylene-ethylene and propylene-1-butene copolymers

Daniela Mileva, René Androsch (✉), Hans-Joachim Radusch

Martin-Luther-University Halle-Wittenberg, Center of Engineering Sciences, 06099 Halle/S., Germany

E-mail: rene.androsch@iw.uni-halle.de; Fax: +49 3461 46 3891

Received: 28 April 2008 / Revised version: 14 July 2008 / Accepted: 3 August 2008

Summary

The effect of variation of the rate of cooling on melt-crystallization of random copolymers of isotactic polypropylene with low amount of either ethylene or 1-butene is evaluated using X-ray techniques, atomic force microscopy, and calorimetry. Slow non-isothermal melt-crystallization mainly results in formation of monoclinic α-crystals of lamellar geometry. The presence of comonomers leads to a decrease of the degree of crystallinity, and of the thickness of lamellae. These changes are proportional to the concentration of co-units, and are more distinct in propylene-ethylene copolymers. Rapid cooling of propylene-1-butene copolymers leads to formation of non-lamellar mesomorphic domains, independent of the concentration of co-units within the investigated range of concentrations. In quenched propylene-ethylene copolymers, in contrast, the formation of mesomorphic structure partially is replaced by formation of monoclinic α-crystals of still non-lamellar geometry.

Introduction

Isotactic polypropylene (iPP) is a semi-crystalline thermoplastic polymer, in which the crystalline phase can adopt different structures [1–4]. These include the monoclinic α-structure, [5] which develops on melt-crystallization in absence of special nucleation agents, the trigonal β-form, [6] which develops preferred in presence of heterogeneous β-nucleators, and the orthorhombic γ-polymorph, [7] which forms on crystallization at elevated pressure, in low-molar-mass fractions, or, being important in the context of the present study, in presence of chain defects [8]. Rapid cooling of the melt inhibits crystallization, if quenching is performed to temperatures lower than the glass transition temperature of the unstrained amorphous phase at about 250 K. Subsequent heating of such a fully amorphous, glassy specimen, or quenching of the liquid to ambient temperature allows formation of mesomorphic structure of rather low packing density, and only two-dimensional order [9–13]. It transforms on heating irreversibly into the monoclinic α-structure, starting at about 350 K [14].

Preparation of random copolymers of propylene with low amount of 1-olefins such as ethylene, 1-butene, 1-hexene, or 1-octene, recently gained increasing interest since it widens the range of potential applications of iPP. A major aspect is the control of the degree of crystallinity and of the crystal size, which, in general, decrease with increasing comonomer content, and affect thermal, mechanical and optical properties [15–19]. The effect of the various types of comonomers on the crystallization behavior of iPP is different, and cannot be generalized. Ethylene units, at best, are only partially included in the crystalline phase, and enrich therefore in the amorphous phase. The ethylene-unit-exclusion process slows down the crystallization, which is manifested by a decreasing crystallization temperature, and a decreasing degree of crystallinity, both being proportional to the concentration of ethylene-defects. In contrast, 1-butene units are more easily incorporated into the crystal, which was concluded from analyses of the lattice constants. The decrease of the degree of crystallinity is therefore less pronounced as in case of ethylene co-units [20,21]. Inclusion of 1-hexene and 1-octene co-units into the crystalline phase seems not favored at concentrations lower than about 10–15 mol-%. There is suggested co-crystallization of propylene and 1-hexene in a new, trigonal crystal form if the concentration of 1-hexene exceeds about 10 mol-% [17,22,23]. Similarly, presence of more than 10–15 mol-% 1-octene results in formation of less ordered mesomorphic crystals of granular texture [16]. Additionally, it was observed that presence of 1-alkene units in the polypropylene chain favors simultaneous formation of α- and γ-polymorphs, with the α/γ ratio depending on the type and concentration of co-units, and on the pathway of crystallization [8,20–26].

The majority of studies about the effect of the chain architecture on structure formation of isotactic propylene-1-alkene copolymers focused on melt-crystallization at low super-cooling or low rate of cooling. We have shown in the past on example of statistical ethylene-1-octene copolymers that the defect concentration in crystals and the formation of specific polymorphs is strongly controlled by the condition of crystallization. In detail we observed replacement of orthorhombic structure with low defect-concentration, which was formed on slow cooling, by pseudo-hexagonal crystals with distinctly higher concentration on 1-octene after rapid cooling of the melt [27–29]. In the present study we attempt therefore to analyze the crystallization of isotactic propylene-ethylene and propylene-1-butene copolymers at high super-cooling, or high rate of cooling, respectively. Fast cooling may result in a partitioning of defects between the crystalline and amorphous phases, which is different from slowly melt-crystallized samples, and which may cause crystallization in different polymorphs. In addition to the analysis of the polymorphism in these copolymers we put special emphasis to the evaluation of the shape and the size of crystals. Recently, we have shown for the iPP homopolymer, that monoclinic lamellae form on non-isothermal melt-crystallization at a rate of cooling lower than about 10^1 – 10^2 K s^{-1}, whereas melt-crystallization at higher rates allowed only formation of mesomorphic nodules. A major result of these studies was the observation of a rather strict relation between crystal structure and crystal morphology. Formation of lamellae seems to be coupled with crystallization into a monoclinic phase, and nodule formation was only observed if mesomorphic structure was detected [30–32]. As far as we are aware of, there are no reports about the morphology of crystals in statistical isotactic propylene copolymers after fast, non-isothermal melt-crystallization, which is therefore a major objective of this initial investigation.

Experimental

Materials

In the present study we used an isotactic polypropylene homopolymer from Montell Polyolefins with a mass-average molar mass and a polydispersity of 373.000 g mol^{-1} and 6.2, respectively. The crystallization behavior, including information about the crystal morphology is described in detail elsewhere [30–34]. Statistical, metallocene-catalyzed, isotactic propylene-ethylene copolymers (iPP-Eth) with ethylene concentrations of 7.4, 12.9, and 17 mol-%, were provided by Dow Europe [35]. The mass-average molar mass and polydispersity of these samples are approximately 110.000 g mol^{-1} and 2.7, respectively. Statistical isotactic propylene-1-butene copolymers (iPP-But) with an average 1-butene content of 6, 9.1, and 10.9 mol-% were purchased from Sigma Aldrich. The mass-average molar mass and the polydispersity of the copolymers with 6 and 10.9 mol-% 1-butene are 225.000 g mol^{-1} and 3.1, respectively. The copolymer with 9.1 mol-% 1-butene has a molar mass of 245.000 g mol^{-1} and a polydispersity of 3.5. Films with a thickness of 100 μm were prepared by compression-molding, using a Perkin-Elmer FTIR film press, with one surface of the samples being in contact with freshly cleaved mica during solidification. Intention of the use of mica as substrate is the generation of a sufficiently smooth surface for subsequent analysis of the structure by atomic force microscopy (AFM). Samples were initially solidified by quenching in ice-water. Crystallization on slow cooling was performed on identical, initially quenched samples, by re-heating into the liquid state and cooling at 10 K min^{-1} with a free surface, using a microscope hot-stage 1350 from Leitz. Additionally, we used a temperature-programmable Collin Press for preparation of slowly crystallized samples of 1 mm thickness.

Instrumentation

Wide-angle X-ray scattering (WAXS) measurements were performed in symmetric transmission mode on an URD 63 diffractometer from Seifert-FPM, using Ni-filtered CuK$_\alpha$ radiation, and a scintillation counter for registration.

Atomic force microscopy (AFM) was done using a Quesant Universal scanning probe microscope, which was equipped with a 5 μm × 5 μm scanner. We used aluminum coated silicon tips NSC14 from MicroMasch, with a force constant of 5 N m^{-1} and a resonant frequency of 160 kHz.

Differential scanning calorimetry (DSC) data were collected with a power-compensation type DSC 7 from Perkin-Elmer. The instrument was operated in conjunction with the cryogenic cooling accessory CCA 7, using liquid nitrogen as coolant. The sample and reference furnaces were purged with gaseous nitrogen at a flow rate of 35 mL min^{-1}. The temperature and heat-flow rate were calibrated following standard procedures, as described in text books [36]. Apparent specific heat capacity data were generated by subtraction of an instrumental baseline, and point-by-point calibration using sapphire as standard. We used 20 μL aluminum pans from Mettler-Toledo for encapsulation of the samples. The sample mass was approximately 3–4 mg. Scanning was performed using rates of temperature-change of 20 K min^{-1} on heating, and 10 K min^{-1} on cooling. For the sake of statistics, additional measurements have been performed on a DSC 820 from Mettler-Toledo.

Results and initial discussion

Wide-angle X-ray scattering (WAXS)

Figure 1 shows WAXS data obtained on slowly melt-crystallized iPP-Eth (a) and iPP-But copolymers (b) of different comonomer concentration, respectively. The concentration of comonomers is indicated in the plots. The two vertical lines in each plot are associated with the 130 peak from α-crystals [1], and with the 117 peak from γ-crystals [7,37]. All other peaks in the investigated angular range may be superpositions of scattering from both crystal phases. The iPP homopolymer crystallizes exclusively in the monoclinic α-phase. Presence of ethylene units results in a decrease of the degree of crystallinity, which is recognized by a distinct decrease of the intensity of the crystalline peaks. Furthermore we observed formation of small amount of orthorhombic γ-structure. Close inspection of the position of the 130 α-crystal peak reveals that the unit cell parameters of the monoclinic crystals apparently are not affected by the presence of ethylene units.

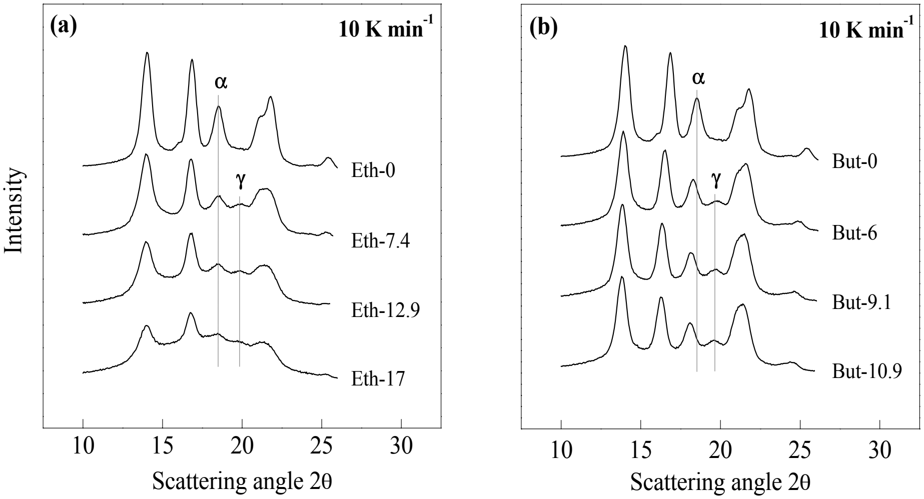

Figure 1. WAXS of iPP-Eth (a), and iPP-But (b) copolymers. Samples were melt-crystallized at a rate of 10 K min^{-1}. Further explanation is given in the text.

The crystallization behavior of iPP-But copolymers is different from that of iPP-Eth copolymers, irrespective similar formation of small amount of γ-structure. First of all, at comparable amount of co-units, the decrease of the degree of crystallinity is much less in case of iPP-But copolymers. Secondly, we recorded a distinct shift of the 130 α-crystal peak to lower scattering angle in iPP-But copolymers, which can be interpreted by an increase of the lattice dimension in direction of the normal of the (130) lattice plane. In other words, 1-butene units may be incorporated to larger extent into the monoclinic unit cell than ethylene co-units. Final evidence for full exclusion of ethylene co-units, however, is not provided with the X-ray data. Experimental NMR data of previous studies suggest partial incorporation of the ethylene units into the crystalline phase [20]. In addition, it has been shown by molecular modeling that ethylene co-units do not largely affect the lateral dimensions of the unit cell [21].

Figure 2 provides a quantitative comparison of the effect of addition of ethylene or 1-butene comonomers on structure formation at slow, non-isothermal melt-crystallization. Figure 2a (left) shows the WAXS-crystallinity, and Figure 2b (right) shows the interplanar spacing of the (130) lattice plane of the monoclinic α-phase, $d_{(130)}$, as a function of the molar percentage of co-units.

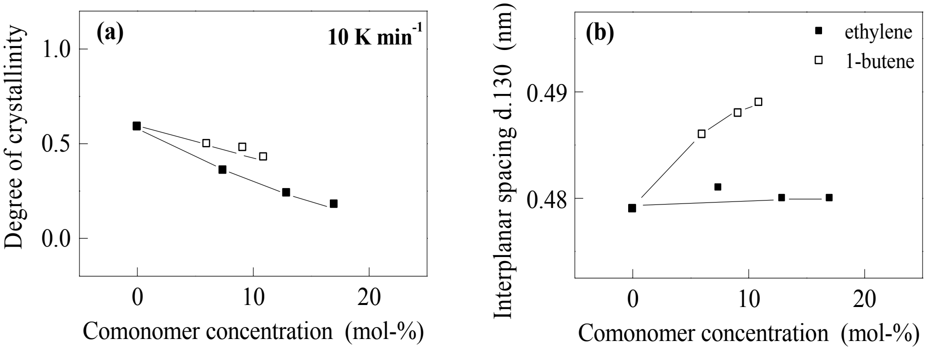

Figure 2. WAXS-crystallinity (a), and interplanar sapcing $d_{(130)}$ (b) of slowly melt-crystallized iPP-Eth (filled squares) and iPP-But copolymers (open squares) as a function of the comonomer concentration.

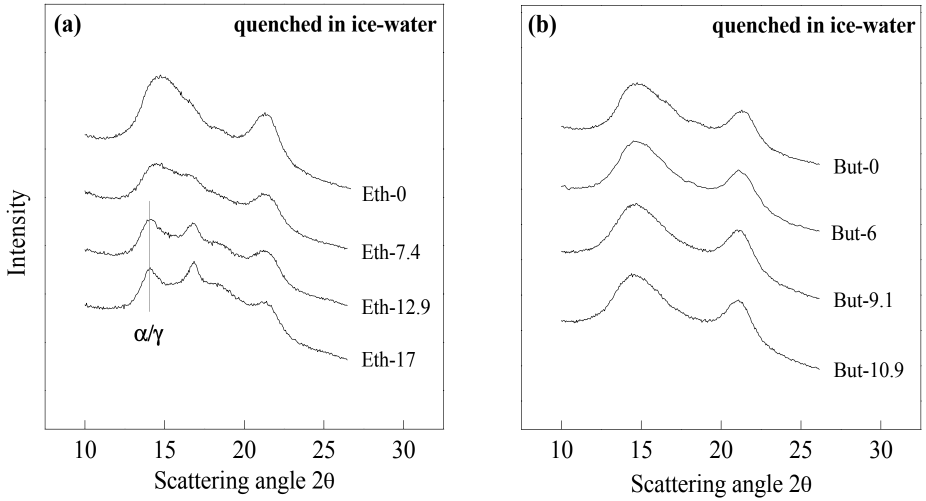

Figure 3. WAXS of iPP-Eth (a), and iPP-But (b) copolymers. Samples were quenched, and subsequently aged at ambient temperature.

Figure 3 shows WAXS data, obtained on samples which were quenched in ice-water, and subsequently stored at ambient temperature. Quenching of the iPP homopolymer results in formation of mesomorphic structure, which is indicated by the typical halo-like scattering maxima. Addition of ethylene co-units suppresses the formation of mesomorphic structure on quenching, and allows formation of low amount of α- or γ-crystals. Due to the low intensity of the reflections, an unambiguous assignment to either monoclinic α-structure, or orthorhombic γ-structure is not possible. In case of addition of 1-butene units, in contrast, formation of monoclinic or orthorhombic crystals is not observed. Instead, mesomorphic structure develops on quenching, as in the iPP homopolymer. The X-ray pattern obtained on quenched iPP-But indicate that the average distance between parallel chains in the mesomorphic structure may slightly be increased. For the iPP homopolymer we calculated from the position of the halo at about 14.6 deg 2θ a distance of 0.605 nm, which coincides with literature data [38–40]. For iPP-But copolymers we observed a linear increase with concentration to reach a maximum value of 0.615 nm in the preparation with 10.9 mol-% 1-butene, indication inclusion of co-units in the mesomorphic phase.

Differential scanning calorimetry (DSC)

Figure 4 shows (a) the onset temperature of crystallization, and (b) the heat of crystallization of iPP-Eth (filled symbols) and iPP-But (open symbols) copolymers. The data were obtained from non-isothermal DSC crystallization experiments, using a rate of temperature-change of 10 K min^{-1}.

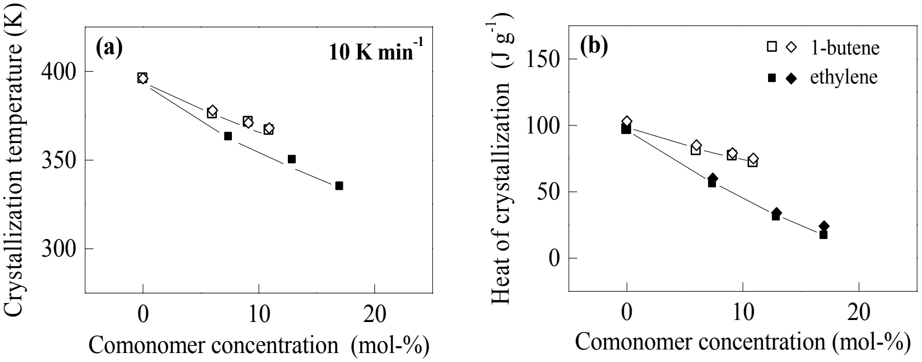

Figure 4. Temperature of crystallization (a) and heat of crystallization (b) of iPP-Eth and iPP-But copolymers, recorded at a rate of temperature-change of 10 K min^{-1}. The square and diamond symbols represent data observed on a DSC 7 and a DSC 820, respectively.

The results allow a rough comparison of the kinetics of crystallization of the different copolymers. Crystallization of iPP, at the specific condition, starts at 398 K. Addition of both ethylene and 1-butene retards the onset of the crystallization process, which is concluded from the lowered crystallization temperature. The decrease of the temperature of crystallization is a function of the comonomer content, and is in iPP-Eth copolymers larger than in iPP-But copolymers. The observation of a larger decrease of the temperature of crystallization in iPP-Eth copolymers indicates a slower kinetics of crystallization, which may be due repelling ethylene units at the crystal growth front, or selection of sufficiently long propylene sequences, respectively. The decrease of the crystallization temperature on addition of comonomers, is paralleled by a decrease of the degree of crystallinity. Note that we did not convert the measured heat of crystallization into an enthalpy-based crystallinity due to unknown bulk specific heat of crystallization. In particular crystals in iPP-But copolymers contain defects which lower the specific heat of crystallization. The heat of crystallization of the iPP homopolymer is close to 100 J g^{-1}, and decreases to 72 J g^{-1} on addition of about 10 mol-% 1-butene. Presence of an approximately identical number of ethylene units decreases the heat of crystallization even to 24 J g^{-1}.

Atomic force microscopy (AFM)

Figure 5 contains AFM images of the iPP homopolymer and iPP-Eth copolymers with different concentration of co-units, as indicated at the bottom. The top images show the structure of specimens which were non-isothermally melt-crystallized at a rate of 10 K min^{-1}, and the bottom images show the structure after quenching in ice-water and aging at ambient temperature. We detected for the samples which were melt-crystallized at a rate of 10 K min^{-1} formation of lamellae (top), with a thickness which decreases with increasing concentration of co-units. Addition of about 7 mol-% ethylene co-units, for instance, results in a decrease of the lamellar thickness from about 20 nm in the iPP homopolymer to about 14 nm. Furthermore, we observed distinct cross-hatching of lamellae [4,41]. The tilt between mother and daughter lamellae is close to perpendicular for the majority of lamellae, which points to dominance of monoclinic α-phase and presence of only negligible amount of γ-crystals, being in agreement with the X-ray data of Figure 1a. Quenching in ice-water, and aging at ambient temperature inhibits formation of lamellae and leads to formation of nodules, at least in surface-near regions. The formation of non-mesomorphic, crystalline structure in samples of higher concentration on ethylene co-units, as detected by WAXS, cannot be identified by AFM. Nonetheless, since the effective cooling rate is lower in the bulk of the films, presence of lamellae in the interior of samples cannot be excluded.

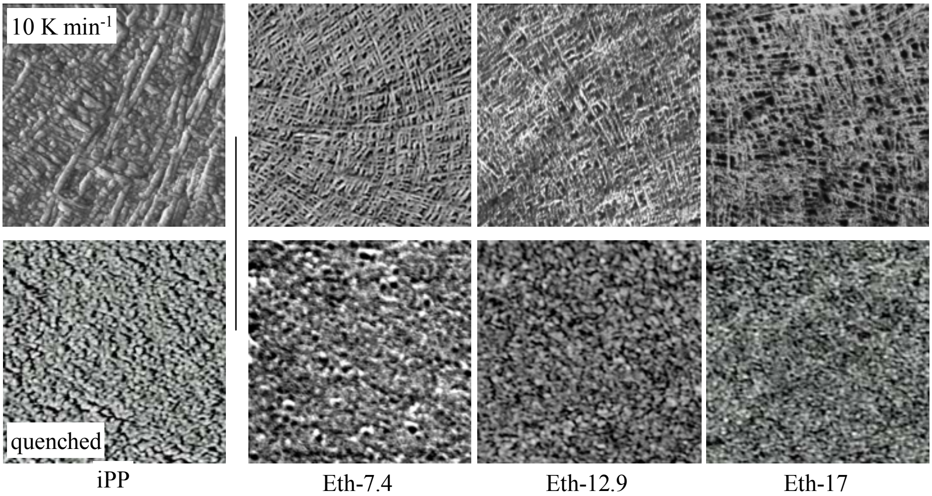

Figure 5. AFM phase-mode images of iPP and iPP-Eth copolymers with different concentration of co-units. The top images were obtained on samples, which were melt-crystallized at a rate of 10 K min^{-1}, and the bottom images were obtained on samples, which were quenched in ice-water and subsequently aged at ambient temperature. The images represent an area of 1×1 μm^2.

Figure 6 shows AFM micrographs of iPP and iPP-But copolymers, which were melt-crystallized at a rate of cooling of 10 K min^{-1} (top), or quenched in ice-water, and aged at ambient temperature (bottom). All images represent an area of 1 μm × 1 μm, and allow therefore a direct comparison with the micrographs of Figure 5. Melt-crystallization at a rate of 10 K min^{-1}, throughout, results in formation of laterally extended, cross-hatched lamellae, with an angle of cross-hatching still close-to-perpendicular, as was also observed in iPP-Eth copolymers. In case of the quenched preparations we observed, regardless the concentration of co-units, non-lamellar particle-like nodules. The size of these domains is about 18–20 nm in the iPP homopolymer, and decreases only slightly to 15 nm in presence of 1-butene co-units. From the X-ray analysis, which is shown with Figure 3, it is known that these nodules are of mesomorphic structure.

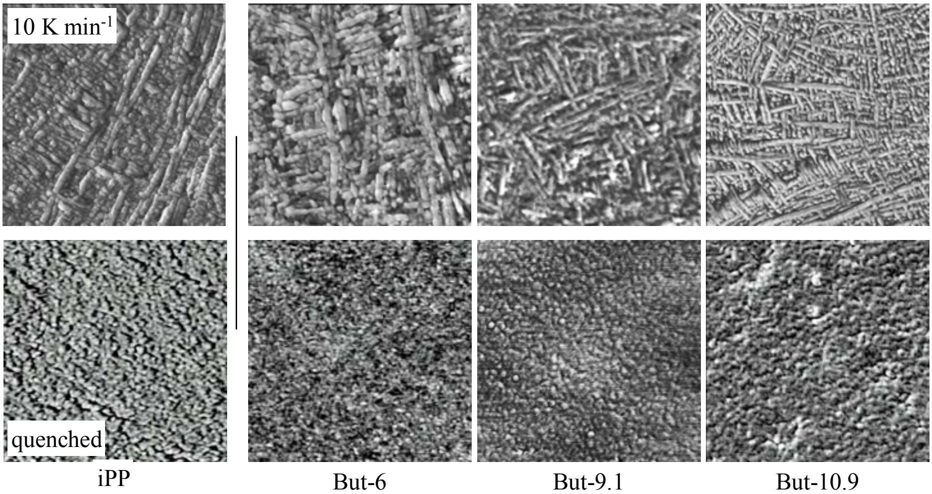

Figure 6. AFM phase-mode images of iPP and iPP-But copolymers with different concentration of co-units. The top images were obtained on samples, which were melt-crystallized at a rate of 10 K min^{-1}, and the bottom images were obtained on samples, which were quenched in ice-water and subsequently aged at ambient temperature. The images represent an area of 1×1 $\mu\mathrm{m}^2$.

Final discussion and conclusions

In the present work we investigated the structure and the structure formation process of statistical isotactic copolymers of propylene with ethylene and 1-butene. Samples were prepared by non-isothermal melt-crystallization applying largely different rate of cooling. The variation of the cooling rate served for initiation of the crystallization process at low and high super-cooling.

WAXS and DSC analyses on rather slowly cooled samples, i.e., of samples which were crystallized at low super-cooling, confirm earlier studies about the effect of ethylene and 1-butene co-units on the crystal structure and degree of crystallinity of iPP [15,20–22,25]. Presence of both ethylene and 1-butene co-units allows formation of α-crystals which coexist with small amount of γ-crystals. Ethylene co-units are not, or to distinctly lower amount incorporated into the crystalline phase than 1-butene co-units. The suggested exclusion of ethylene co-units from the crystallization delays the kinetics and reduces the degree of crystallinity stronger than in case of 1-butene units, which are incorporated into the crystals.

An exclusion of ethylene co-units from crystallization may be caused by unfavorable loss of the symmetry of the chain in the monoclinic α-crystal. It has been found, based on molecular modeling, that ethylene units may produce either an inversion of the chirality of the 3_1 helix in combination with a bending of the chain, or a straight chain without affecting the chirality of the chain before and after the defect. It is suggested in the literature that only the bent conformation can easily be incorporated into the γ-crystal or the α/γ-disordered modifications. In case of 1-butene, in contrast, the symmetry of the chain is not affected as much as in case of ethylene-units. The 1-butene unit does not locally alter the helix-conformation and affects only the lateral dimensions of the crystal [21].
The temperature of crystallization decreases on addition of co-units (Figure 4a) which is in the following explained by a decrease of the equilibrium melting temperature. The equilibrium melting temperature of the monoclinic α-crystal of the iPP homopolymer is reduced in random copolymers due to changes of the specific enthalpy and/or entropy of melting. We estimated the melting point depression with the Flory equation [42] (eq 1), which implies full exclusion of co-units from crystallization, and with the Sanchez-Eby equation [43] (eq 2), which allows to consider partial inclusion of co-units into the crystal:

$$\frac{1}{T_m^0} - \frac{1}{T_{m,c}^0} = \frac{R}{\Delta H_m^0} \ln X \tag{1}$$

$$\frac{1}{T_m^0} - \frac{1}{T_{m,c}^0} = -\frac{R}{\Delta H_m^0} \left\{ \frac{\varepsilon X_c}{R\, T_{m,c}^0} + (1 - X_c) \ln\left[\frac{1 - X_c}{1 - X}\right] + X_c \ln\left[\frac{X_c}{X}\right] \right\} \tag{2}$$

$T_{m,c}{}^0$ and $T_m{}^0$ (=460.7 K [44]) are the equilibrium melting points of the copolymer and of the homopolymer, respectively, R is the gas constant, $\Delta H_m{}^0$ (=8.7 kJ mol^{-1} [44]) is the specific heat of fusion of the crystal, and X is the total molar fraction of co-units. X_c is the fraction of co-units in the crystalline phase, increasing the Gibbs free energy of the crystal by εX_c. Note that the Sanchez-Eby equation (eq 2) simplifies to the Flory-equation (eq 1), if X_c is zero. Figure 7 shows the equilibrium melting temperature of iPP-Eth and iPP-But copolymers as a function of the comonomer concentration. The squares were calculated with eq (1), assuming full exclusion of co-units from crystallization. The melting point depression would in this case be independent of the type of copolymer. However, for iPP-But copolymers we detected an almost linear increase of the lateral dimension of the unit cell, which points to inclusion of co-units into the crystal, and which requires application of eq (2) for estimation of the equilibrium melting point depression. The stars were calculated by eq (2), using a partitioning ratio X_c/X of 0.5, independent on the comonomer concentration, and using an excess free energy ε of 2.94 kJ mol^{-1} [45].
The calculated equilibrium-melting-point data serve for explanation of the decrease of the crystallization temperature which is different for iPP-Eth and iPP-But copolymers. The data of Figure 7 show that the equilibrium melting point depression is larger in iPP-Eth copolymers. Consequently, from thermodynamic point-of-view, lower crystallization temperatures are expected on addition of ethylene co-units, in comparison to the addition of equivalent amount of 1-butene units. The experimentally observed temperatures of crystallization, shown in Figure 4a, confirm the prediction based on the calculation of the equilibrium melting temperature.

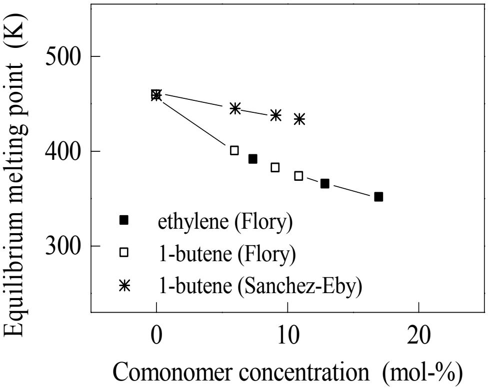

Figure 7. Equilibrium melting points of iPP-Eth and iPP-But copolymers as a function of the comonomer content. Calculations were done using eqs (1) and (2), as described in the text.

Further progress of analysis of the structure of random iPP-Eth and iPP-But copolymers is provided in this work with the application of AFM for evaluation of the crystal morphology. We consider the AFM data, which were obtained on slowly cooled preparations as completion of former research, which was done on samples of different comonomer concentration, and different thermal history [15,20,46]. Direct microscopic analysis of the crystal morphology of isothermally crystallized copolymers with rather high concentration on ethylene co-units of 14.7 mol-%, or more, revealed an axialitic/lamellar crystal habit, and a crystal thickness which, within the limits of the particular investigation, is almost independent on the crystallization temperature, and on the concentration on ethylene co-units [20]. A comparison of these literature-data with crystal thicknesses obtained in the present study is provided with Figure 8. In general, there is observed a decrease of the thickness of lamellae with increasing concentration on ethylene or 1-butene co-units. Furthermore, the decrease of the thickness of lamellae in iPP-But copolymers seems slightly less than in iPP-Eth copolymers of identical molar percentage of co-units.

Formation of lamellae, in the investigated range of concentration on co-units, is not observed on crystallization at high super-cooling. The AFM-images of copolymers which were crystallized between 273 and 298 K (bottom row in Figures 5 and 6) show a nodular structure, independent on type and concentration of co-units. The size of nodules is about 18–20 nm in the homopolymer. Addition of co-units is not connected with a qualitative change of the crystal morphology, and the size of nodules is, at best, reduced by a few nanometers. The formation of nodules on rapid cooling of iPP is well-documented in the literature. In general, it can be assumed that the non-lamellar shape of crystals/domains probably arises from the large number of nuclei which form at low temperature, limiting lateral crystal growth.

With the present study we prove for the first time that nodule formation also occurs in iPP-Eth and iPP-But copolymers if crystallization is enforced at sufficiently low temperature. We detected formation of mesomorphic structure in iPP-But copolymers, similar as in the iPP-homopolymer (Figure 3b). In contrast, crystallization of iPP-Eth copolymers with about 10–20 mol-% ethylene resulted in additional formation of small amount of α- or γ-crystals (Figure 3a). The different tendency of iPP-Eth and iPP-But copolymers for formation of α- or γ-crystals at identical condition of crystallization, and at comparable amount of co-units must be attributed to a stronger depression of the equilibrium melting point of monoclinic/orthorhombic crystals in iPP-Eth copolymers (see Figure 7). As a consequence, super-cooling to activate crystallization of monoclinic/orthorhombic crystals at ambient temperature is for iPP-Eth copolymers lower than for iPP-But copolymers. A lower equilibrium melting temperature of monoclinic crystals in iPP-Eth copolymers can be explained with exclusion of co-units from crystallization, which affects the equilibrium melting point depression stronger than in case of partial incorporation of co-units. The observation of increasing fraction of α/γ-crystals with increasing comonomer content in quenched iPP-Eth preparations (Figure 3a), supports the above discussion.

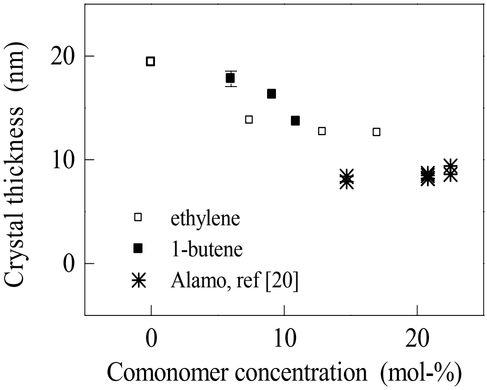

Figure 8. Crystal thickness of iPP and iPP-Eth and iPP-But copolymers as a function of the comonomer concentration. The squares represent data of this work, as derived from the AFM images of the top row in Figures 5 and 6. Literature-data (stars) are included for comparison.

Acknowledgment. The research was supported by a grant from the EU SOKRATES/ERASMUS program for one of authors (D.M.). Furthermore we acknowledge financial support by the Deutsche Forschungsgemeinschaft (DFG). We thank DOW Europe GmbH for providing the propylene-ethylene copolymers.

References

1. Turner-Jones A, Aizlewood JM, Beckett DR (1964) Makromol Chem 75:134
2. Addink EJ, Beintema J (1961) Polymer 2:185
3. Keith HD, Padden Jr. FJ, Walter NM, Wyckoff HW (1959) J Appl Phys 30:1485
4. Lotz B, Wittmann JC, Lovinger AJ (1996) Polymer 37:4979
5. Natta G, Corradini P (1960) Nuovo Cimento Suppl 15:40
6. SV Meille, DR Ferro, S Brückner, AJ Lovinger, Padden FJ (1994) Macromolecules 27:2615
7. Brückner S, Meille SV (1989) Nature 340:455
8. Zimmermann HJ (1993) Macromol Sci, Phys B32:141
9. de Santis F, Adamovsky S, Titomanlio G, Schick C (2006) Macromolecules 39:2562
10. Hsu CC, Geil PH, Miyaji H, Asai K (1986) J Pol Sci, Pol Phys 24:2379
11. Caldas V, Brown GR, Nohr RS, MacDonald JG, Raboin LE (1994) Polymer 35:899
12. Miyamoto Y, Fukao K, Yoshida T, Tsurutani N, Miyaji H (2000) J Phys Soc Jap 69:1735
13. Natta G (1960) Makromol Chem 35:40
14. Zannetti R, Celotti G, Fichera A, Francesconi R (1969) Makromol Chem 128:137

15. Stephens CH, Poon BC, Ansems P, Chum SP, Hiltner A, Baer E (2006) J Appl Pol Sci 100:1651
16. Poon B, Rogunova M, Chum SP, Hiltner A, Baer E (2004) J Pol Sci, Pol Phys 42:4357
17. Poon B, Rogunova M, Hiltner A, Baer E, Chum SP, Galeski A, Piorkowska E (2005) Macromolecules 38:1232
18. Poon BC, Dias P, Ansems P, Chum SP, Hiltner A, Baer E (2007) J Appl Pol Sci 104:489
19. De Rosa C, Auriemma F, di Capua A, Resconi L, Guidotti S, Camurati I, Nifantev IE, Laishevtsev IP (2004) J Am Chem Soc 126:17040
20. Jeon K, Chiari YL, Alamo RG (2008) Macromolecules 41:95
21. De Rosa C, Auriemma F, Ruiz de Ballesteros O, Resconi L, Camurati I (2007) Macromolecules 40:6600
22. De Rosa C, Iacono SD, Auriemma C, Ciaccia E, Resconi L (2006) Macromolecules 39:6098
23. De Rosa C, Auriemma F, Ruiz de Ballesteros O, De Luca D, Resconi L (2008) Macromolecules 41:2172
24. Alamo RG, Kim MH, Galante MJ, Isasi JR, Mandelkern L (1999) Macromolecules 32:4050.
25. Hosier IL, Alamo RG, Esteso P, Isasi JR, Mandelkern L (2003) Macromolecules 36:5623
26. Foresta T, Piccarolo S, Goldbeck-Wood G (2001) Polymer 42:1167
27. Androsch R (1999) Polymer 40:2805
28. Androsch R, Blackwell J, Chvalun SN, Wunderlich B (1999) Macromolecules 32:3735
29. Androsch R, Kolesov I, Radusch HJ (2003) J Therm Anal Cal 73:59
30. Zia Q, Androsch R, Radusch HJ, Piccarolo S (2006) Polymer 47:8163
31. Zia Q, Radusch HJ, Androsch R (2007) Polymer 48:3504
32. Zia Q, Androsch R, Radusch HJ, Ingolič E (2008) Polymer Bulletin 60:791
33. Androsch R, Wunderlich B (2001) Macromolecules 34:5950, ibid. 34:8384
34. Androsch R (2008) Macromolecules 41:533
35. personal communication, Dow Europe GmbH, 2007
36. Wunderlich B, Thermal Analysis of Polymeric Materials, Springer, Berlin, 2005
37. Meille SV, Brückner S, Porzio W (1990) Macromolecules 23:4114
38. Zannetti R (1984) Polymer Bulletin 11:533.
39. Natta G, Peraldo M, Corradini P (1959) Rend Accad Naz Linzei 26:14
40. Mc Allister PB, Carter TJ, Hinde RM (1978) J Pol Sci, Pol Phys 16:49
41. Lotz B, Wittmann JC (1986) J Pol Sci, Pol Phys 24:1541
42. Flory PJ (1949) J Chem Phys 17:223
43. Sanchez IC, Eby RK (1975) Macromolecules 8:638
44. Bu HS, Cheng SZD, Wunderlich B (1988) Makromol Chem, Rapid Comm 9:75
45. Alamo RG, Ghosal A, Chatterjee J, Thompson KL (2005) Polymer 46:8774
46. Hosier IL, Alamo R, Lin JS (2004) Polymer 45:3441